



Article

Comparison of Satellite Platform for Mapping the Distribution of Mauritius Thorn (*Caesalpinia decapetala*) and River Red Gum (*Eucalyptus camaldulensis*) in the Vhembe Biosphere Reserve

Farai Dondofema ^{1,*}, Nthaduleni Nethengwe ¹, Peter Taylor ² and Abel Ramoelo ³

¹ Department of Geography and Environmental Sciences, University of Venda, Thohoyandou 0950, South Africa

² Department of Zoology & Entomology, University of Free State, Phuthaditjhaba 9866, South Africa

³ Centre for Environmental Studies, Department of Geography, Geoinformatics and Meteorology, University of Pretoria, Hatfield, Pretoria 0083, South Africa

* Correspondence: farai.dondofema@univen.ac.za; Tel.: +27-765004979

Abstract: Mapping and tracking invasive alien plant species (IAPS) and their invasiveness can be achieved using remote sensing (RS) and geographic information systems (GIS). Continuous monitoring using RS, GIS and modelling are fundamental tools for informing invasion and management strategies. Using systematic comparisons, we look at three remote sensing imagery platforms and how accurately they can be classified within the Vhembe biosphere reserve, Limpopo Province, South Africa. Supervised classification of National Geospatial Information Colour Digital Aerial Imagery, DigitalGlobe Worldview 2 and CNES SPOT 6 was performed. The Spectral Angle Mapper (SAM) algorithm was used to identify the best satellite for species-level classification. The accuracy of the classifications produced an overall accuracy (OA) of 71% with a Kappa coefficient (KC) of 0.76 for CDA photographs, an OA of 81% and a KC of 0.80 for Worldview 2, and an OA of 89% with a KC of 0.86 for SPOT 6 imagery. Therefore, SPOT 6 imagery came out as the most suitable for species-level classification. The classification results from the SPOT 6 imagery were used as input data for further species distribution modelling of Mauritius Thorn and River Red Gum in the VBR.

Keywords: classification; remote sensing; GIS; producer accuracy; user accuracy; overall accuracy; Kappa coefficient



Citation: Dondofema, F.; Nethengwe, N.; Taylor, P.; Ramoelo, A. Comparison of Satellite Platform for Mapping the Distribution of Mauritius Thorn (*Caesalpinia decapetala*) and River Red Gum (*Eucalyptus camaldulensis*) in the Vhembe Biosphere Reserve. *Remote Sens.* **2023**, *15*, 2753. <https://doi.org/10.3390/rs15112753>

Academic Editors: Gaofei Yin, Justin F Moat, Jean-Philippe Gastellu-Etchegorry, Baodong Xu and Shengbiao Wu

Received: 12 March 2023

Revised: 4 May 2023

Accepted: 24 May 2023

Published: 25 May 2023



Copyright: © 2023 by the authors. Licensee MDPI, Basel, Switzerland. This article is an open access article distributed under the terms and conditions of the Creative Commons Attribution (CC BY) license (<https://creativecommons.org/licenses/by/4.0/>).

1. Introduction

1.1. The Invasive Alien Species Problem

Nearly all ecosystems on Earth have problems associated with invasive alien plant species (IAPS). The invasions of these species into natural systems pose a challenge to the functioning of global biodiversity, habitats and economic costs [1]. Invasive alien plant species detection processes are usually localised. Remote sensing (RS) and geographic information systems (GIS) thus have the potential to contribute toward high mapping accuracies for use by both the scientific and management communities [2]. Complemented by field-based techniques, RS and GIS can simultaneously map and monitor larger scales [3]. RS and GIS provide potentially valuable resources for mapping and tracking IAPS and provide data inputs to models that predict areas vulnerable to invasion [2,4]. These technologies can be regarded as cost-effective and wide-ranging, providing the ability for long-term reporting and monitoring of IAPS are recognised as basic research needs [2].

Presence records derived from RS and GIS can be used to create permanent records that could easily be used as inputs into ecological models for management and control activities [5,6]. The availability of multitemporal RS data makes it possible to predict trends leading to efficient monitoring of abundance and distribution patterns over time [7].

Using the presence data of IAPS from RS and GIS allows monitoring and mapping of areas susceptible to invasion, thus, enabling the set-up of preventive measures that can accurately deal with problematic species [8]. RS and GIS techniques can effectively map locations at risk of invasion. Alternatively, upon the establishment of IAPS, RS and GIS can be used to map potential invasion pathways.

1.2. The Use of GIS and RS in Identifying IAPS

For the effective use of RS and GIS in identifying and monitoring IAPS, it is essential to understand the characteristics of the IAPS at the species level and their surroundings [9]. RS and GIS can then be used to map and monitor IAPS based on the ability to discriminate between IAPS and surrounding species, e.g., an understory species whose direct detection is from RS and GIS [10,11]. RS and GIS detection approaches rely on plant phenological, biochemical, structural and observable spatial patterns as IAPS proliferate in the vegetative canopy.

1.2.1. Aerial Photography

When selecting imagery to map IAPS, aerial photography is cheap and provides acceptable spatial resolution (0.1–2 m). The high spatial resolution of aerial photos meets most criteria for sampling IAPS to satisfy management interest, even when considering small patch sizes, albeit only for some understory species that do not form distinct patches. Aerial photography is thus considered suitable when the IAPS exhibit visual traits that separate them from surrounding vegetation.

Based on its characteristic pale yellow flower, aerial photography was utilised to detect the Mauritius Thorn [12]. Many woody invasives, including blackberry (*Rubus fruticosus*), European olive (*Olea europaea*), and Pinus species, have previously been mapped using high-resolution colour infrared aerial photography [13]. Using visual and computer-assisted digital colour infrared photographs analysis, invasive *Vachellia* species were efficiently mapped from surrounding indigenous plants and South Africa's fynbos habitat [14].

While high spatial resolution aerial photography can be affordable, visual processing takes time, making interpretation difficult in most instances since it requires both ability and experience [15]. In addition, field measurements must be appropriately calibrated to find spectral variations in the target species rather than capturing photos of surrounding plants. Due to these restrictions, data can only be collected in relatively limited geographical areas.

1.2.2. Multispectral Imagery

Multispectral imaging is based on sensors that measure reflected energy within several specific bands, varying from 3 to 10 bands across the electromagnetic spectrum. For example, SPOT images were used to identify Cogon grass (*Imperata cylindrica*) infiltrating savanna habitats [16]. In Nepal's lowland forests, Landsat ETM+ data were utilised to indirectly map IAPS in the understory based on the density of forest canopies and the intensity of light penetrating the understory [17]. Multispectral imaging outperforms aerial photography. However, some of the most common and economically important IAPS may be intermingled with other species or have thin canopies that make distinction difficult.

1.3. Trade-Offs Between Image Resolution and Mapping Accuracy

The mapping accuracy of IAPS-infected vegetation communities is highly influenced by spatial and spectral resolution. Even though systematic comparisons of several sensors across the same spatial region are critical for understanding temporal changes, there are few clear instances of IAPS, providing no direction to explain the selection of suitable sensors for invasion. While mapping IAPS in South African riparian habitats, researchers noticed that visual interpretation using 1:10,000 panchromatic aerial photos produced the most accurate results [18]. Landsat 8 imagery resulted in lower accuracy [19]. This is mainly because of the accessibility and affordability compared to hyperspectral techniques.

Research findings in South Africa indicated that Colour Infrared Red images, a form of aerial photographs with a more excellent spectral resolution, produced higher accuracy [20]. Furthermore, when comparing imagery with various spatial and spectral resolution combinations, results indicate higher mapping accuracies for IAPS with distinct features beyond the visible spectrum, with better spectral resolution than spatial resolution.

The well-known trade-off between spectral and spatial resolution and data picture processing costs complicates choosing the suitable image resolution even further (Figure 1). Although a comparison of analysis of multispectral (Landsat 8) with moderate resolution imagery from SPOT and aerial photos for a 100 km² study area [21,22] points to Landsat ETM+, CDA and SPOT 6 to be the cheapest as they are freely available, with DigitalGlobe Worldview 2 imagery the most expensive, there have been few systematic cost comparisons of RS and GIS in comparable research locations.

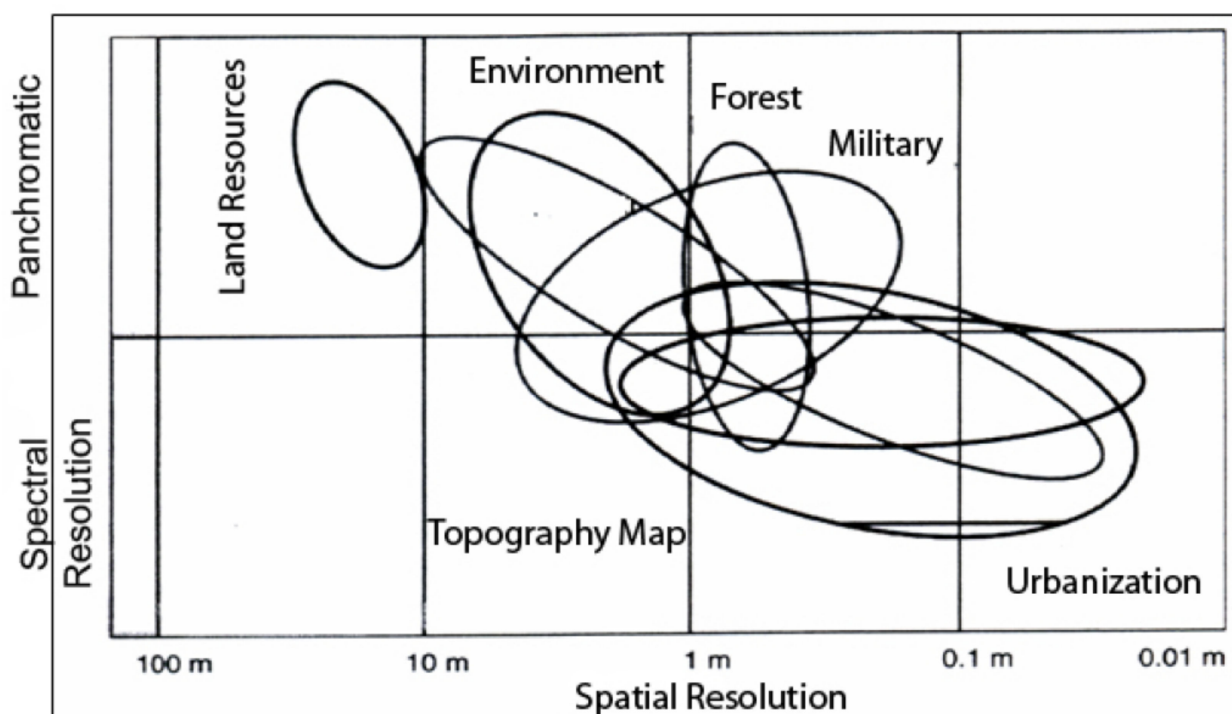


Figure 1. Relationship between spectral, spatial resolutions and usage type [23].

1.4. Identifying the Potential Distribution of Invasive Alien Species

While not a replacement for rigorous systematic field surveys, distribution models may be a viable option for estimating IAPS distribution [24]. As a result, prioritising precious resources such as people, time and cash for control and monitoring is accelerated [25]. The bulk of prediction models is statistical, with the presence or presence-absence data used to infer environmental circumstances that comprise most of the presence locations [26]. Remotely sensed variables such as vegetation, atmosphere, soil, geomorphology, proximity to roads or pathways and knowledge of management practices may be predictors in most environmental niche models (ENM). Mechanistic models are used to simulate physiologically limiting elements in a species' tolerance to the environment [27–29]. In correlative species distribution models, environmental factors are statistically linked to species occurrence or abundance [30]. On the other hand, process-based models establish a species' ecology as mathematical functions that define causation; the species' presence or abundance is an indirect, emergent result [30]. The mechanistic niche model uses comprehensive biophysical modelling tools to understand species distribution [31].

The spread of IAPS presents a complex and costly problem to most countries [32]. Typical characteristics of IAPS include fast growth, expansion, massive distribution, phenotypi-

cal plasticity, survival in different forms of foods and various environmental conditions [33]. A good indicator of invasion depends on a species' success in invading a new area [34]. Therefore, remotely sensed images should be coupled with indirect mapping methods, including the use of GIS data layers and modelling [35]. In the case of IAPs that occur in the vegetation canopy, successful detection approaches have generally capitalised on unique phenological or biochemical properties, structural characteristics or spatial patterns created by invasions. It is thus essential to provide a brief synopsis of phenological or biochemical properties and structural features that can be used to map IAPs successfully. The potential for regional invasion in South Africa was examined locally using climatic envelope models for 71 IAPS and existing presence data collected at a geographical resolution of 25 km [36]. To identify invasion hotspots for several species, there has been a shift toward an alternate method to multiple species modelling [37].

Indirect Identification of Areas Vulnerable to Invasion Using RS and GIS

RS and GIS can detect landscape and site features, making mapping IAPS distribution possible [38]. RS and GIS can be used to identify regions with excessive rates of deforestation that can result in plant invasions by integrating propagule transportation and micro-disruption (it should be acknowledged that defoliation due to grazing can also affect IAPS) [39]. The ability to detect changes in the terrain over time may be used to define disturbance regions prone to invasion. Land degradation of the natural environment means edge ecosystems are more vulnerable to plant invasions than core ecosystems [40]. The spatial distribution of natural habitats in images and degradation indices can help identify invasion-prone locations.

1.5. Limitations of RS Applications to IAPS

For more accurate species distribution and risk maps, there is a need to complement MaxEnt with Generalised Linear Mixed Models (GLMMs) to identify areas of possible spread for conservation purposes [41]. Ref. [42] modelled hotspots of IAPs through Ecological Niche Modelling (ENM) using MaxEnt to guide the formulation of an effective policy for controlling the IAPs. The area under the curve (AUC) scores obtained for predictions can be sufficiently accurate [43]. However, SDMs have some limitations, such as overestimation of the presence of species. The assumption of a random sampling of species' existence on the grid cells made by SDMs predicts each cell's significant probability of fact, which could be overestimated [44].

The high data, software and hardware costs significantly impact the uses of RS and GIS in monitoring IAPS; this is typical for contemporary high-resolution images. However, notable trends are showing declining imagery costs, such as the free access provisions being given by Landsat [45]. Technical expertise is required to process images (visual interpretation) and multispectral (image processing). As indicated by comparing aquatic and terrestrial ecosystems, the ability to map IAPS and the accuracy with which they may be identified changes between environments [46,47]. When spatial data and satellite images are integrated with field measurements, the best classification results are produced, giving vital inputs for classifying and validating image classifications. Because of a better grasp of plant phenology and its implications on spectral resolution, practical awareness and familiarity with the environment enhances classification accuracy significantly.

Notwithstanding the constraints above, remote sensing remains the most significant approach for effectively gathering information across broad regional extents at high spatial resolution while allowing for the most significant percentages of spatial sampling. Developments in remote sensing, such as increased temporal image acquisition and approaches that combine passive, radar and thermal sensors and texture analysis, will almost certainly expand the resources available to map IAPS. The trade-offs between satellite image resolution continuously shift as remote sensing technologies advance and new data sources become accessible. Policies governing access to remote sensing data are evolving; a casing point is the benefit of high-resolution imagery in structured, searchable, well-documented libraries

locally and globally. The South African National Space Agency (SANSA) and other governmental satellite datasets have made great strides in earth observation data democratisation in South Africa. This study aimed to evaluate the accuracy of the NGI-CDA, DigitalGlobe Worldview 2 and CNES SPOT 6 for species-level plant species discrimination.

2. Materials and Methods

2.1. Study Region

The research site discussed falls within the VBR. The VBR is a member of the World's Reserve Network organised by Man and Biosphere (MAB, UNESCO), located in the northern part of South Africa, covering five local municipalities of the Limpopo Province (Blouberg, Collins Chabane, Makhado, Musina, and Thulamela). International borders to the north and east include Botswana, Zimbabwe, and Mozambique. This site was selected due to the invasion by River Red Gum and Mauritius Thorn and the contrast in climatic conditions.

The VBR covers an area of 3,070,000 ha (30,701 km²), including part of the Kruger National Park (KNP) north of the Shingwedzi River. The Mogalakwena River forms the eastern border. The southern boundary spans from south of the Blouberg–Makgabeng and Soutpansberg Mountain range to the east, over the Luvuvhu River catchment. The VBR lies between the following coordinates (23°30'S and 22°14'S and 28°45'E and 31°29'E). Within the VBR, the altitude ranges from 2500 m above mean sea level (asl), 719 m asl (Hangklip) and 1748 m asl (Lajuma).

The extreme maximum and minimum temperatures recorded in the VBR are 43.2 °C and −3.4 °C [48]. The winters in the VBR are generally mild, and frost sometimes occurs only in the southern valleys [49]. In Entabeni, the highest observation station in the region, the average seasonal rainfall surpasses 850 mm, and occasionally the total annual rainfall may exceed 2000 mm. On the other hand, stations in the mountain's rain shadow or low-lying locations, such as Pafuri and Alldays, receive barely 200 to 300 mm of seasonal rain. However, because of the area's poor rainfall measurement network, local fluctuations cannot be precisely assessed.

The VBR's bushveld vegetation unit of the savannah biome is officially classified as vulnerable. The bushveld vegetation unit comprises a rainfall gradient distribution of thick deciduous woods and evergreen montane forests, with a weakly established grassy layer and open savannah in certain areas. In addition, exotic eucalyptus and pine plantations on the Soutpansberg range further strained the Soutpansberg Mountain bushveld vegetation unit's survival. In general, vegetation groups in the Soutpansberg Mountains appear in east–west bands along the easterly moisture flow from the Indian Ocean, following the direction of the mountain range's ridges.

The VBR consists of three biomes: savanna, grassland and forest, as well as four bioregions and twenty-three distinct plant types or biotopes. South Africa is home to eight of these biotopes. The region is also a bio-geographical node, comprising the Kalahari and Lowveld bioregions with mild to tropical temperatures. This produces zones of biologically significant interactions, which must be safeguarded for conservation to be viable. Based on a combined examination of species, ecosystems and biological processes, the South African National Spatial Biodiversity Assessment (NSBA) has designated the Blouberg and Soutpansberg complex as one of nine priority sites for conservation efforts [50]. Additionally, it is the same region as a biodiversity and endemism hotspot in South Africa.

2.2. Land-Cover Classes and Invasive Alien Plant Species

Twelve land-use/land-cover classes were classified, including two genera of invasive alien trees. The identified land-use/land-cover classes: (i) Unclassified, (ii) Water, (iii) Buildings, (iv) Bare Area, (v) Road, (vi) Plantation, (vii) Orchard, and (viii) Forest.

A McNemar test was run to test the difference between the three satellite platforms used in the land-cover classification. This was performed through a nonparametric test that

compared the classification results from the three satellite platforms with binary responses for randomised complete blocks.

2.3. Datasets

This study used classification and accuracy assessment methods using colour digital aerial imagery (CDA), Worldview 2 and SPOT 6 imagery. All the image analysis was performed using ENVI 5.3 and ESRI's ArcGIS 10.8.1 software. A summary of the imagery used in this study is presented in Table 1.

Table 1. Specifications of the satellite data used in this study.

Sensor	Scene	Date of Acquisition	Resolution (m)	Spectral Bands
CDM aerial photographs	2329BB	2018-07-16	0.25	Blue, Green, Red
	SPOT6_20181102_13303316qth9fssm80h_2	2018-11-02	8 m	Blue (0.455 μm –0.525 μm)
2018-11-02		8 m	Green (0.530 μm –0.590 μm)	
2018-11-02		8 m	Red (0.625 μm –0.695 μm)	
2018-11-02		8 m	Near-Infrared (0.760 μm –0.890 μm)	
Worldview 2	012969746010_01_003	2017-05-12	1.8 m	Coastal: 400–450 nm
	012969746010_01_003	2017-05-12	1.8 m	Blue: 450–510 nm
	012969746010_01_003	2017-05-12	1.8 m	Green: 510–580 nm
	012969746010_01_003	2017-05-12	1.8 m	Yellow: 585–625 nm
	012969746010_01_003	2017-05-12	1.8 m	Red: 630–690 nm
	012969746010_01_003	2017-05-12	1.8 m	Red Edge: 705–745 nm
	012969746010_01_003	2017-05-12	1.8 m	Near-IR1: 770–895 nm
	012969746010_01_003	2017-05-12	1.8 m	Near-IR2: 860–1040 nm

2.4. Training Data

Training data were gathered using two sources of information: (i) ecological input on target groups and (ii) field surveys (Table S1) [51]. These training data were used to produce the classifications, which were ground-truthed using locations highlighted in Table S2. In addition, a local ecological expert was engaged to provide coordinates and shapefiles of infestations of these target invasive alien plant groups. During the field surveys, an effort was made to obtain a reasonable spatial spread of points across classes, with a specific focus on the Soutpansberg mountains and the Luvuvhu Valley (Figure 2). For each land-cover class, there are 7271 points for 12 classes.

2.5. Classification

Classification of images is a means of decryption of satellite images, identification and delineation of any objects on the image. Classification can also be defined as a process of automatic decryption. The classification algorithms are divided into two classes according to user involvement: unsupervised (pixel-based classification and essentially computer-automated classification) and supervised (spectral signatures obtained from training samples to classify an image) classification. Supervised classification was performed on the CDA, SPOT 6 and Worldview 2 images to differentiate the various vegetation types in the study area. Each pixel in an image is assigned to a group or class in the pixel-based classification process. Then, using spectral pattern recognition, each pixel is allocated to a

class based on its spectral properties. Object or feature-based classification methods use what is known as feature space to classify the pixels. Feature space is a scatter plot of the two bands' spectral values for all the image's pixels. Because the classes in this study are land-cover, the purpose is to map the land-cover types throughout the image. This study collected ground reference land-cover information during the three field sampling excursions in June–July 2019 and February 2020.

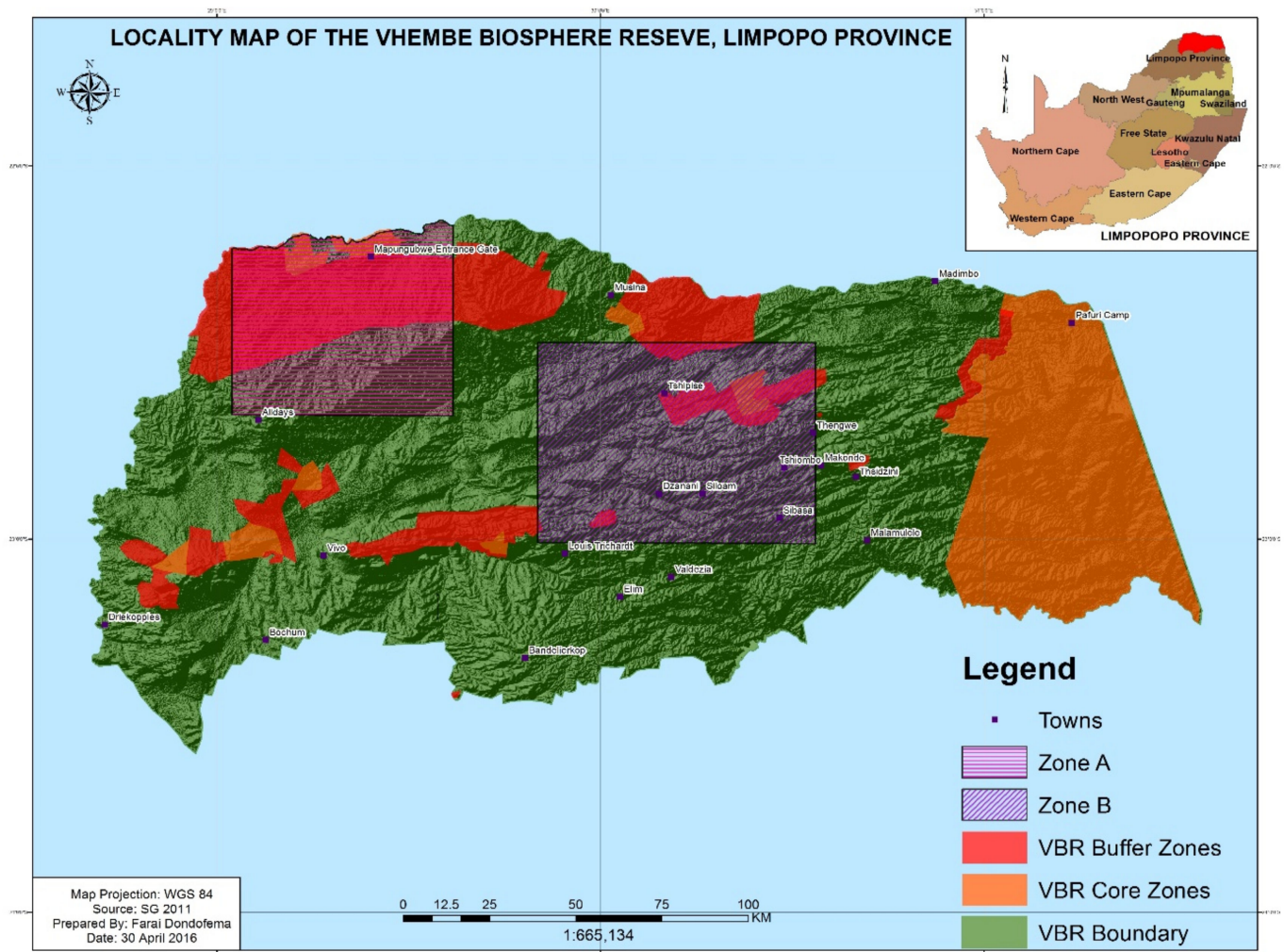


Figure 2. Locality Map of Vhembe Biosphere Reserve in the Limpopo Province [52].

2.6. Supervised Classification

Supervised classification aims to extrapolate land-cover type information from a known segment of a remotely sensed image using data acquired during fieldwork to unknown areas of the whole image. As a result, for each land-cover category, the analyst defines many 'training' regions. Based on this information, the computer develops spectral signatures using specialised spatial analysis tools. The maximum likelihood descriptor is the most common method to measure the spread of values around the mean of the class. Each image pixel is allocated to one of the groups covered by the land as far as feasible by the spectral signature. ENVI 5.3 software used for classification in this study has four different classification algorithms to choose from when running the supervised classification procedure. These include Minimum Likelihood Distance (MLD), Mahalanobis Distance and Spectral Angle Mapper (SAM). The SAM method was chosen because of its ability to compute the spectral angle between an image spectrum and a reference spectrum using vectors in n-dimensional spectral space, where n is the number of bands

and reduces the influence of shading effects to emphasise the intended reflectance qualities [53]. SAM is also a simple and quick approach for mapping picture spectral similarity to reference spectra.

Figure 3 shows the supervised classification process.

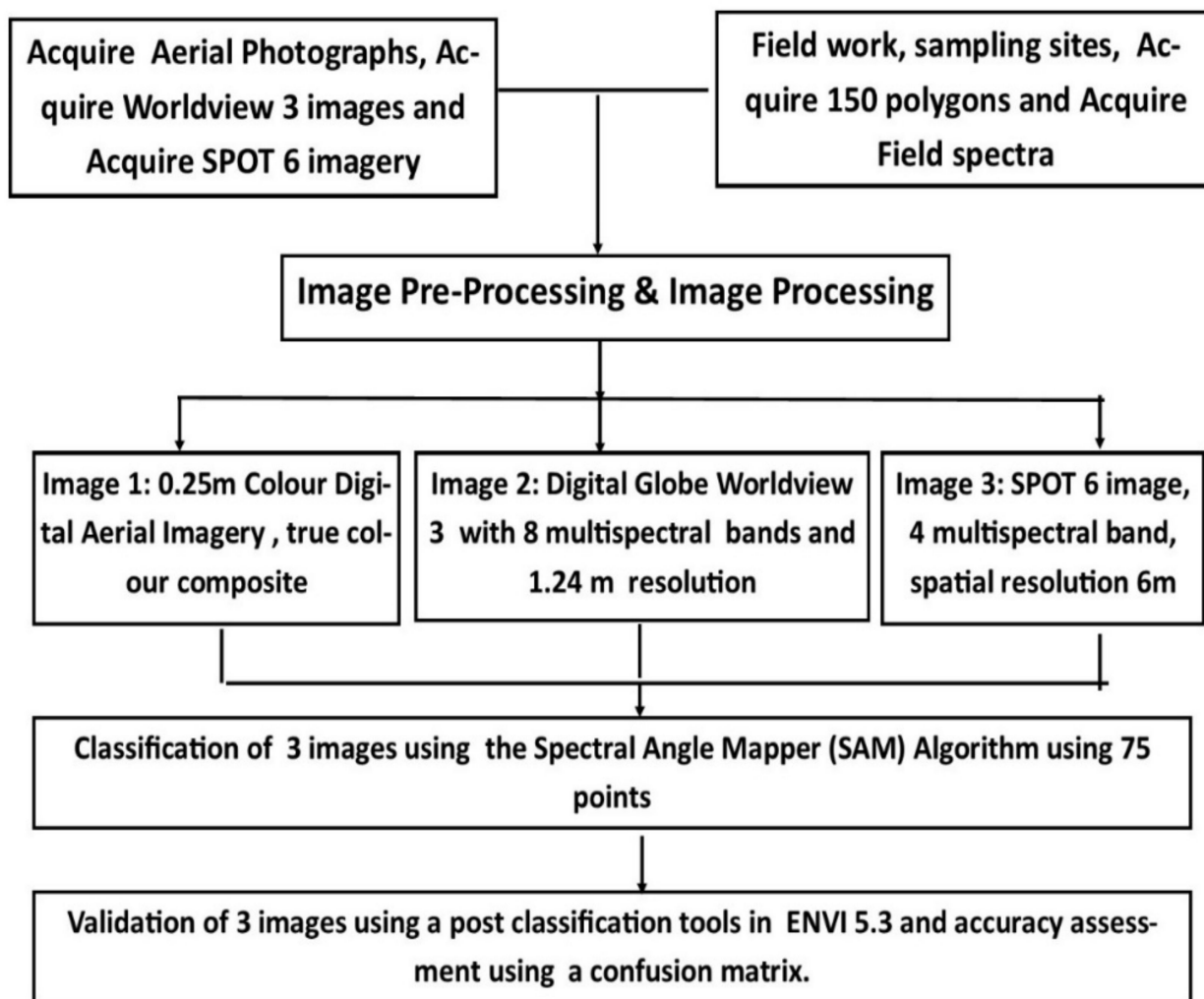


Figure 3. Classification of CDA, Worldview 2 and SPOT 6 datasets.

After visually assessing many classification approaches in Environment for Visualising Images (ENVI 5.3) (Exelis Visual Information Solutions, 2013), the spectral angle mapper (SAM) classifier was chosen for our purposes because of its more remarkable ability to recognise active vegetation. The SAM is a supervised machine learning approach that uses statistical learning theory to achieve classification. The SAM classifies data by extracting a hyperplane from a multidimensional feature space that optimally divides classes. This hyperplane is the ideal decision surface for class separation. The ideal hyperplane maximises the margin, which is the distance between the hyperplane and the nearest positive and negative training examples. The optimisation problem is addressed using training samples to discover the hyperplane, resulting in a sparse solution. Even though the SAM is a binary classifier in its most basic form, the SAM classifier implementation in ENVI was enlarged to more than two classes by breaking the problem down into a series of binary class separations [54].

Several kernels, including the polynomial, radial basis function and sigmoid, may classify SAM in ENVI to represent more complicated forms than linear hyperplanes. The SAM was used with the radial basis function kernel for paired classification. During training,

the SAM classifier can additionally implement a penalty parameter for misclassification. The penalty parameter was set to its maximum value, whereas a classification probability threshold of zero was used to classify all pixels [55]. For picture classifications, the classifier's default settings were utilised. During the classification phase, the spectral subset option in ENVI was used to select only the NIR band of the NAIP imagery.

The approach taken in this study is to assess all three images (CDA photograph, Worldview 2 and SPOT 6) individual performance to classify land covers in the study area and evaluate their errors and accuracy to select the imagery with the highest accuracy for species-level extraction.

Accuracy Assessment of CDA, Worldview 2 and SPOT 6 Classification

Classification accuracy was evaluated by developing an error matrix for each classified image that analyses the relationship between reference categories on the ground and matching classified categories on the image group-by-group basis. By comparing the identified classes to the ground verification data, error matrices for each classification map were constructed. To assess classification accuracy, error matrices were generated, which included overall, producer and user accuracies. Using site verification data, field validation (accuracy evaluation) was undertaken (ground control points). Verification data for 175 sites were randomly generated using the "Generate Random Sample Using Ground Truth Image in the post-classification tool" function in ENVI 5.3 software.

The verification points were loaded into a real-time differential Trimble GeoXH Global Positioning System (Trimble Navigation Limited, Sunnyvale, CA, USA) outfitted with the ArcPad software package, a 4 m external antenna, providing submeter horizontal accuracy (10 cm), and navigated at sites before image classification. This resulted in an unbiased field validation technique based on visited sites without prior knowledge of whether the classification method had demarcated areas for the relevant land-cover groups. Next, the land-cover type in the 175 regions was evaluated and allocated to GPS locations. Following the classification of the images, these locations were placed on the land-cover map, and a one-to-one matching was performed to create an error matrix for each site.

The error matrix was used to calculate the accuracy evaluation for classified maps, individual land-cover classes and the kappa coefficients and variances. To compare image classification at 95% confidence level sites, a two-tailed Z-test ($Z/2 = Z_{0.025}$) was used. The kappa statistic calculates the degree of agreement or accuracy between the classification map obtained from images and the ground verification data. When the row and total column estimations are considered, this is characterised by the significant diagonal and the chance agreement. For example, the Kappa values for CDA, Worldview 2, and SPOT 6 classification vary from 0 to 1, with values more than 0.80 indicating high agreement between the categorised map and ground truth, and values less than 0.40 indicating poor agreement—scores ranging from 0.40 to 0.80 show moderate agreement with the underlying data.

3. Results

3.1. Extraction of Training Samples from the Colour Digital Aerial Imagery

The spatial coverage of the Colour Digital Aerial (CDA) is illustrated in Figure 4 within the study area. Bare lands are distinguished by a lighter reddish tone on the CDA composite image, herbaceous vegetation by a greyish response (with intermittent stream segments) and water by black or blue tones. Figure 4a reveals distinct spatial patterns of plantations, forests, orchards, water, bare area and other land-cover classes on each site. Image classification resulted in 3.49% Unclassified, 36.21% Buildings, 6.28% Plantations, 20.81% Forest, 2.83% Tar and 11.17% water. With a kappa value of 0.757, the overall accuracy of land-cover classifications was 70.50%.

3.2. Extraction of Training Samples Digital Globe Worldview 2 Imagery

The spatial coverage of the Worldview 2 imagery is illustrated in Figure 5 within the study area. Figure 5a shows the Digital Globe Worldview 2 Imagery with 1.24 m images for sites. The actual colour composite imagery reveals distinct spatial patterns of plantations, forests, orchards, water, bare area and other land-cover classes on each site. Plain regions are distinguished by a light greyish tone, herbaceous plants with a dark green response, and water with brown or blue tones in the actual colour composite image. Image classification resulted in 35.92% Unclassified, 0.22% BuiltUp Area, 25.51% Plantation, 34.91% Forest, 0.53% Road and 0.43% Water. Land-cover classes were identified with an overall accuracy of 80.50% with the associated kappa coefficient of 0.80.

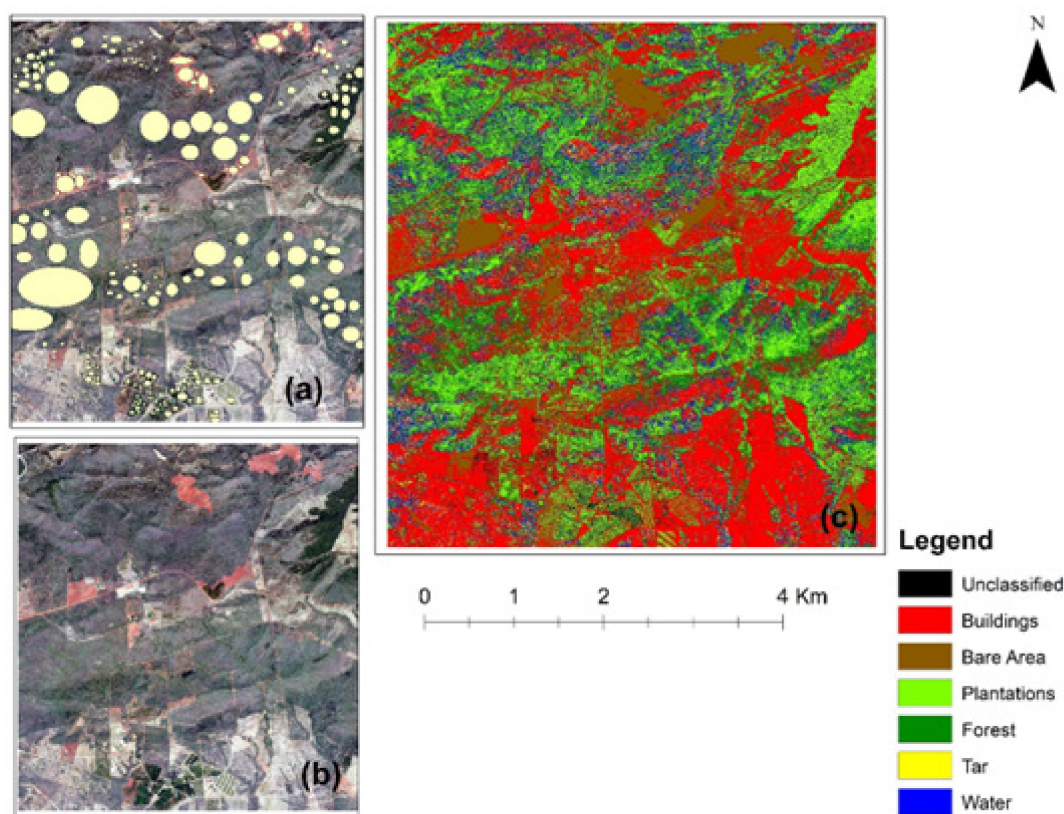


Figure 4. The colour digital aerial with 0.25 m spatial resolution and validation polygons represented with (a) yellow dots, while (b) is the true colour imagery, and (c) is the classified aerial imagery for the study site.

3.3. Extraction of Training Samples SPOT 6 Imagery

The spatial coverage of the SPOT 6 imagery is illustrated in Figure 6 within the study area. Figure 6a shows the SPOT 6 Imagery; the true colour composite imagery reveals distinct spatial patterns of plantations, forests, orchards, water, bare area and other land-cover classes on each site. The SPOT 6 composite image shows that a brownish tone, herbaceous plants with a light green response and water with blue tones characterise bare regions. Image classification resulted in 23.39% Unclassified, 0.820378% Water, 1.50% Buildings, 13.66% Bare Area, 7.88% Road, 5.47% Plantation, 12.72% Orchard and 34.55% Forest. The associated kappa coefficient of 0.857 was used to identify land-cover classes with an overall accuracy of 88.89%.

The McNemar test is used to see if there are differences between two related groups in a dichotomous dependent variable. It is similar to the paired-samples *t*-test, except that the dependent variable is dichotomous rather than continuous.

The null hypothesis cannot be rejected because the computed p -values from the McNemar test for the three remote sensing platforms are greater than the significance level $\alpha = 0.05$. The alternative hypothesis that the classification results from the three remote sensing platforms differ cannot be accepted because the computed p -values from the McNemar test are more significant than the significance level $\alpha = 0.05$.

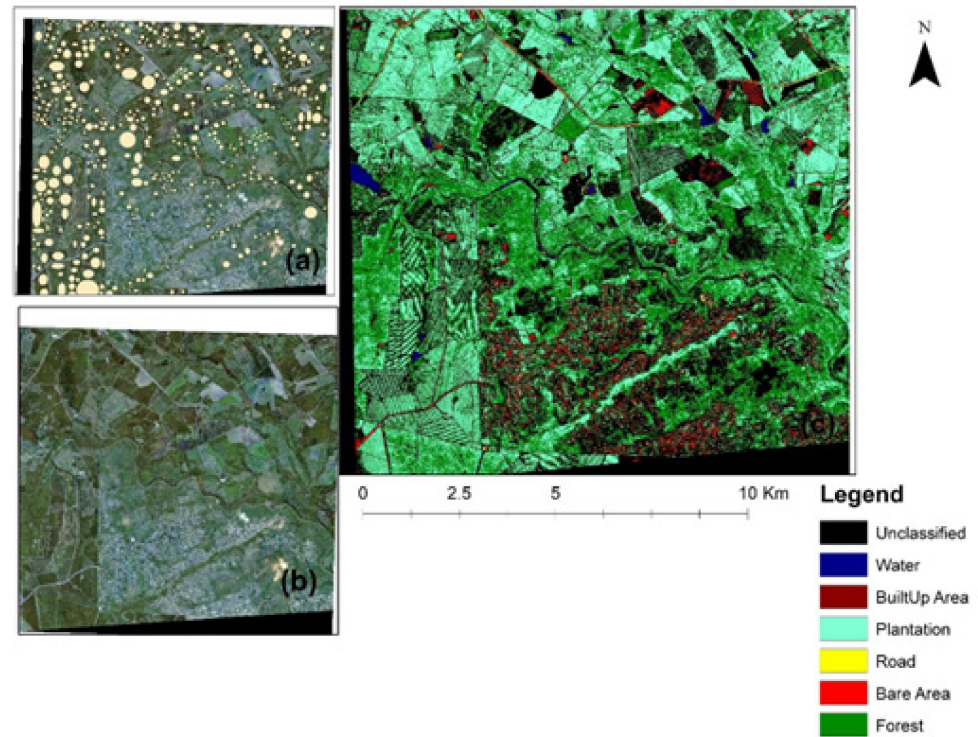


Figure 5. The Digital Globe Worldview 2 Imagery with 1.24 m spatial resolution and validation polygons represented with (a) yellow dots, while (b) is the colour imagery, and (c) classified Worldview 2 imagery for the study site.

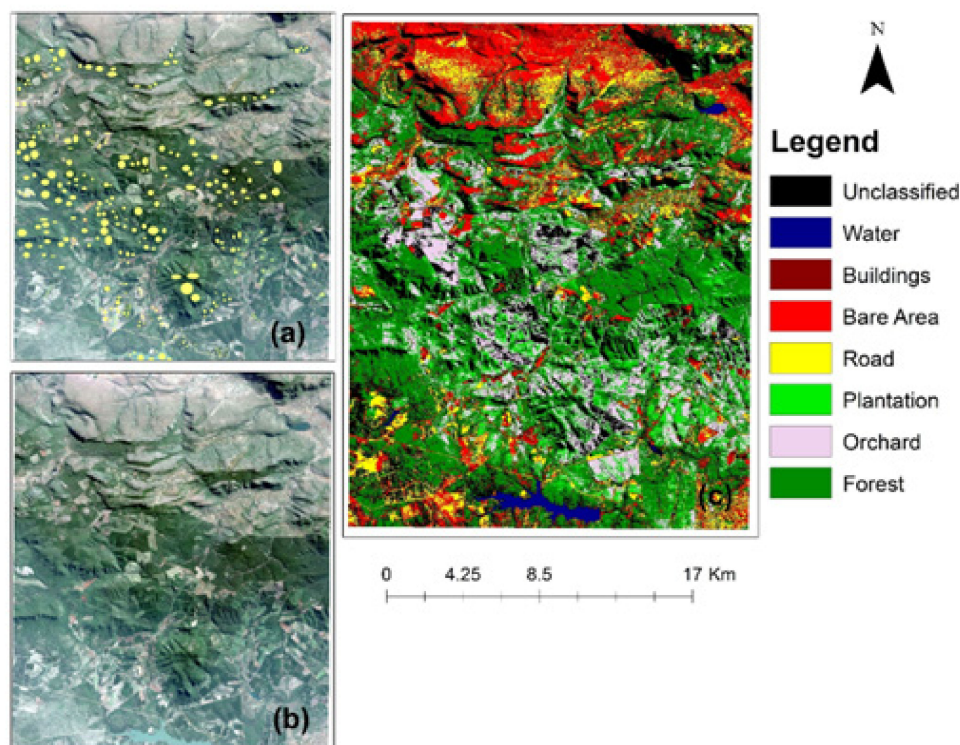


Figure 6. The SPOT 6 imagery with 6 m spatial resolution and validation polygons represented with (a) yellow dots, (b) is the colour imagery, and (c) is the classified SPOT 6 imagery for the study site.

3.4. Species-Level Extraction of Training Samples from SPOT 6 Imagery

After running classification, validation and accuracy assessment of the three sets of images (The DigitalGlobe Worldview 2, NGI aerial photographs and CNES Spot 6 images), the results indicated that the SPOT images produced the best classification with high levels of accuracy with 87.50%, 87.50% and 88.89% respectively. Given this backdrop, Spot 6 satellite images of Mauritius Thorn and River Red Gum were chosen for species-level classification. Furthermore, based on the spectral difference between living vegetation (forest, plantation, orchard) and senescent herbaceous or nonvegetative components, the 6 m multispectral SPOT 6 satellite images enabled unambiguous identification of all prevalent land-cover classes (paved road, shadow, exposed soil, water).

The spatial coverage of the SPOT 6 imagery is illustrated in Figure 6 within the study area. Figure 6 shows the SPOT 6 Imagery with 6 m spatial resolution for sites. The true colour composite imagery reveals distinct spatial patterns of plantations, forests, orchards, water, bare area and other land-cover classes on each site. For example, on the SPOT 6 composite image, bare regions are characterised by brownish tones, herbaceous plants by a light green response and water by blue tones. Table 2 summarises the classification analysis, while Table 3 shows the classification performance.

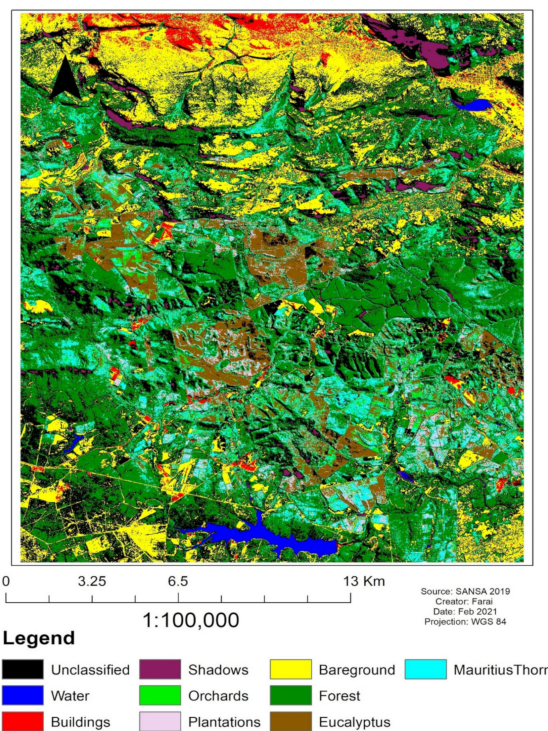
Table 2. Systematic comparison using the McNemar test.

	WV-NGI	SPT-NGI	WV-SPT
Q	3.200	2.250	0.500
z (Observed value)	1.789	1.500	0.707
z (Critical value)	1.960	1.960	1.960
p-value (Two-tailed)	0.074	0.134	0.480
alpha	0.05	0.05	0.05

Table 3. The cover classification performance for the three data products.

Classification	Overall Accuracy (Percent)	Kappa Coefficient	User Accuracy (Percent)	Producer Accuracy (Percent)
NGI-CDA	88	0.8571	100	94
DigitalGlobe-Worldview 2	88	0.8571	100	94
CNES-SPOT 6	89	0.875	100	94
Species Level CNES-SPOT 6	89	0.857	87	86

Image classification resulted in 23.69% Unclassified, 0.82% Water, 2.91% Buildings, 17.47% Bare ground, 1.26% Shadows, 2.91% Plantation, 2.48% Orchards, 33.03% Forest, 6.60% Eucalyptus and 8.84% Mauritius Thorn. Land-cover classes were identified with an overall accuracy of 88.89% and an associated kappa coefficient of 0.8750. The producer's accuracy ranged from 50% for unclassified to 100% for water, while the user's accuracy varied from 50% for unclassified water to 100% for water (Figure 7). At a 95% confidence level, the Z-statistics (1.75 3.15) revealed an insignificant difference in the site classifications. A close look at the field-collected spectral, presence and absence data illustrates that, in most cases, the Mauritius Thorn occurred as mixed pixels within the natural vegetation. At the same time, the River Red Gum grew as homogeneous assemblages close to plantations or abandoned plantations.

**Figure 7.** The SPOT 6 Imagery with 6 m spatial resolution and validation points represented with classified aerial imagery for the study site.

4. Discussion

Using a timely, low-cost method, accurate information may be obtained about the current distribution of Mauritius Thorn and River Red Gum across large, challenging areas. This information can then be used in several types of rangeland ecology and management sectors. This study investigated the effectiveness of using three satellite platforms based on their spatial and spectral resolution, classification and statistical results from the McNemar test to enable further species distribution modelling of the IAPS.

It was feasible to discern the characteristics appearing in an image in terms of the object or type of land cover these features truly represent on the ground using supervised classification, making image classification the most significant element of digital image analysis. However, the results also show that it is not the image platform with the finest spatial resolution that performs best in classification; it is also necessary to consider the spectral resolution.

Using three imagery sets in the study shows how remote sensing for IAPS detection has advanced rapidly. It progressed from CDA and photo interpretation approaches to digital image processing, with machine learning replacing manual interpretation to discover small characteristics the human eye cannot detect. Remote sensing technology advancements have resulted in less expensive and faster methods of managing forest resources. Nonetheless, there are still limitations to their widespread use in IAPS monitoring. Monitoring, detection and reporting on forest health concerns have constantly been prioritised by the Department of Forestry, Fisheries and the Environment (DFFE), Endangered Wildlife Trust (EWT) and Working for Water (WfW), particularly in protected areas such as the VBR. The rate of forest area conversion inside the VBR, human-caused changes in land cover, and the threat of IAPS introduction and establishment have all heightened the demand for improved near-real-time tools and commodities.

A variety of stakeholders must be included throughout the process to maximise the usefulness of the established classification:

- Rather than just receiving letters of support, end users and other important stakeholders should be involved in the experimental design from the start;
- The researcher selected and visited practitioners in the study region at prospective field sites for data collection;
- Including stakeholders in fieldwork, learning from their experience, and instilling a feeling of ownership in the project increased the likelihood of final product identification and adoption.

This was performed to avoid the restricted cooperation required for this study among land managers, practitioners and decision-makers. The classification results in the study region of Eastern Soutpansberg using the SPOT 6 image identified that 336 hectares were covered by Mauritius Thorn and 2629 hectares were covered by River Red Gum. In comparison, the SPOT 6 image covered a total area of 35,765 hectares. A notable pattern was with River Red Gum, with which 11 most 30% of the identified trees were located close to plantations. In comparison, approximately 25% had escaped along watercourses, with the remainder (45%) being found all over the area of interest.

The management goals inform the spatial scales at which the classification technique can be adopted within the VBR [56]. Field-based surveys will always obtain the most detailed and accurate information about IAPS. As a result, researchers may conduct on-site measurements of foliar chemistry, canopy structure and spectral features. Nonetheless, it is crucial to stress that the relevance of this study in advising management across the larger environment is restricted. The operational scale is also suggested for imaging with high spatial and spectral resolution, which is perfect for detecting IAPS. Unfortunately, such initiatives may be geographically constrained because of the high cost and computational requirements. The recent addition of enhanced satellite sensors (e.g., Worldview 2 and SPOT 6) has dramatically increased the capability to cover large areas at higher spatial resolutions. However, global evaluations of forest conditions often necessitate decreased spatial resolution to analyse information over enormous geographic extents. Mixed pixels, which are far more effective, frequently disguise slight changes in vegetation conditions. However, they might be helpful in time series analysis when focusing on relative changes in vegetation indicators at continental sizes.

The scope of the inquiry determines the optimum technique for mapping and modelling the spread of IAPS, the amount of information required for the available resources, and the period if the research was to be upscaled from the VDM to the Limpopo area of South Africa. In that case, the assessment criterion may have to sacrifice spatial and

spectral resolution (as well as predictive detail and accuracy) to attain the needed geographic coverage. On the other hand, a municipality worried about the propagation of a freshly identified IAPS may forego broad regional coverage to maximise the spatial and spectral resolution required to identify specific, newly developed IAPS. As with this study, some typical constraints are accessible images, time and financial resources. Gathering high-resolution pictures after September 2012 using the SPOT 6 satellite data is difficult. However, historical broadband satellite images (SPOT 1, 2, 3, 4 and 5) may provide a general evaluation of former circumstances dating back to 1986.

The comparison of CDA, Worldview 2, and SPOT 6 imagery demonstrated that, even when not adequately suited to the user's demands, diverse satellite images may give insight that traditional monitoring cannot. The results from this study have also raised that the most comprehensive approach to detecting novel IAPS issues can only be achieved by combining several methods. One good example is the harmonisation of the SPOT 6 and Worldview 2 images to improve the resolution of the resultant output. In investigating the three satellite platforms, the best method was to investigate the relationship between spectral characteristics from higher-resolution imagery that might be utilised to train coarser-resolution data for a larger-scale review. The key is to recognise that there is no single correct strategy and that various remote sensing technologies may be employed to meet goals. According to the classification findings, SPOT 6 images performed better than aerial and Worldview images.

Many factors influence the capacity of SPOT 6 images to assess trends and patterns in woody plant cover. The spatial, spectral and radiometric resolutions, as well as the image scale, image processing methods, atmospheric haze, shadow, terrain effects, the angle between the sensor and the vegetative layers, the relative contrast between the vegetative layers and the background, canopy architecture, crown size and height and plant density, all have a significant impact on the detection capabilities of remotely sensed images. When canopies of individuals of the same or different plants overlap, it is impossible to discern whether a particular image shows one giant plant, numerous plants of the same species or various plants of different species from a top-down perspective.

5. Conclusions

Remote sensing and GIS techniques provide unique methods for recognising and mapping plant species. They can characterise the scope of an invasion by differentiating the invading species from the rest of the vegetation mosaic in a timely and spatially specific manner. The SAM classifier detected the two IAPS: Mauritius Thorn and River Red Gum. Given these woody plant invasions' economic and ecological ramifications, the results show that SPOT 6 imagery has the best accuracy when mapping the extent of various vegetation types and invasions.

Except for little mapping plants with less than 1 m diameter canopies, the 6 m scale level of precision proved appropriate in mapping both Mauritius Thorn and River Red Gum. A higher-resolution photograph of these plants may be required. This might be significant if the aim is to identify the early phases of invasion with juvenile plants. These maps may be used to monitor and plan management efforts for both under study. The SAM classifier's capacity to correctly identify diverse plant species has advantages in assessing biomass levels of each species and determining the quantity and kind of treatments necessary for woody invasion mitigation, which might differ for different shrub species. This study demonstrates how to use SPOT 6 images with a spatial resolution of 6 m to evaluate infestation by undesired rangeland species. This approach and technology should be explored when high-scale maps are required for study or land management.

The SPOT 6 archive has been operational since September 2012, providing nine years of historical analysis. The CDA images have great promise; unfortunately, the restricted spectral resolution prevents precise classification from being used to its full potential. Nevertheless, when comparing the classification accuracy of the three images, it was clear that the CDA photographs had a Kappa coefficient of 0.757 (substantial strength of

agreement), Worldview 2 had a Kappa coefficient of 0.80 (substantial strength of agreement), and SPOT 6 imagery had a Kappa coefficient of 0.857 (almost perfect strength of agreement). This is confirmed further by the findings of a thorough comparison of the three remote sensing platform classification results, which reveal considerable variances between the platforms for remote sensing.

Supplementary Materials: The following supporting information can be downloaded at: <https://www.mdpi.com/article/10.3390/rs15112753/s1>.

Author Contributions: F.D.: Investigation, Data curation, Formal analysis, Writing—original draft; P.T.: Conceptualization, Investigation, Methodology, Resources, Data curation, Supervision, Writing—initial draft; A.R.: Conceptualisation, Methodology, Data curation, Formal analysis, Writing—original draft; N.N.: Investigation, Writing—review and editing. All authors have read and agreed to the published version of the manuscript.

Funding: We greatly acknowledge the University Staff Doctoral Programme (USDP), the University of Venda Capacity Development Towards a Higher Degree (D020) and DigitalGlobe Foundation DGF—Farai Dondofema Sales Order Number: 0056549303.

Data Availability Statement: The datasets generated and analysed during this study are not publicly available as they are part of a more extensive study that is currently ongoing but are available from the corresponding author upon reasonable request.

Acknowledgments: Tinkham (Forest Biometrics Lab) and Miranda Redmond (Forest and Wood-land Ecology Lab) in the Department of Forest and Rangeland Stewardship for hosting me at the University of Colorado during my research.

Conflicts of Interest: The authors declare no conflict of interest.

References

1. Clusella-Trullas, S.; Garcia, R.A. Impacts of invasive plants on animal diversity in South Africa: A synthesis. *Bothalia-Afr. Biodivers. Conserv.* **2017**, *47*, 1–12. [[CrossRef](#)]
2. Asner, G.P. Tropical forest carbon assessment: Integrating satellite and airborne mapping approaches. *Environ. Res. Lett.* **2009**, *4*, 034009. [[CrossRef](#)]
3. Issa, S.; Saleous, N. Modeling the Environment with Remote Sensing and GIS: Applied Case Studies from Diverse Locations of the United Arab Emirates (UAE). In *Geographic Information Systems and Science*; IntechOpen: London, UK, 2018; p. 81.
4. Melesse, A.M.; Weng, Q.; Thenkabail, P.S.; Senay, G.B. Remote Sensing Sensors and Applications in Environmental Resources Mapping and Modelling. *Sensors* **2007**, *7*, 3209–3241. [[CrossRef](#)]
5. Beccari, E.; Carmona, C.P.; Tordoni, E.; Petruzzellis, F.; Martinucci, D.; Casagrande, G.; Pavanetto, N.; Rocchini, D.; D’Antracoli, M.; Ciccarelli, D.; et al. Plant spectral diversity from high-resolution multispectral imagery detects functional diversity patterns in coastal dune communities. *bioRxiv* **2023**. [[CrossRef](#)]
6. Pinto-Ledezma, J.N.; Cavender-Bares, J. Predicting species distributions and community composition using satellite remote sensing predictors. *Sci. Rep.* **2021**, *11*, 16448. [[CrossRef](#)]
7. Cord, A.F.; Meentemeyer, R.; Leitão, P.J.; Vaclavik, T. Modelling species distributions with remote sensing data: Bridging disciplinary perspectives. *J. Biogeogr.* **2013**, *40*, 2226–2227. [[CrossRef](#)]
8. Leitão, P.J.; Santos, M.J. Improving Models of Species Ecological Niches: A Remote Sensing Overview. *Front. Ecol. Evol.* **2019**, *7*, 9. [[CrossRef](#)]
9. Pinto-Ledezma, J.N.; Cavender-Bares, J. Using Remote Sensing for Modeling and Monitoring Species Distributions. In *Remote Sensing of Plant Biodiversity*; Springer: Cham, Switzerland, 2020; pp. 199–223. [[CrossRef](#)]
10. Serbin, S.P.; Townsend, P.A. Scaling Functional Traits from Leaves to Canopies. In *Remote Sensing of Plant Biodiversity*; Springer: Cham, Switzerland, 2020; pp. 43–82. [[CrossRef](#)]
11. Bolch, E.A.; Santos, M.J.; Ade, C.; Khanna, S.; Basinger, N.T.; Reader, M.O.; Hestir, E.L. Remote Detection of Invasive Alien Species. In *Remote Sensing of Plant Biodiversity*; Springer: Cham, Switzerland, 2020; pp. 267–307. [[CrossRef](#)]
12. Everitt, J.H.; Anderson, G.L.; Escobar, D.E.; Davis, M.R.; Spencer, N.R.; Andrascik, R.J. Use of Remote Sensing for Detecting and Mapping Leafy Spurge (*Euphorbia esula*). *Weed Technol.* **1995**, *9*, 599–609. [[CrossRef](#)]
13. Crossman, N.; Kochergen, J. Mapping environmental weeds in the Mount Lofty Ranges, South Australia, using high resolution infrared aerial photography. In Proceedings of the 13th Australian Weed Conference, Mitcham, Australia, 8–13 September 2002.
14. Stow, D.; Hope, A.; Richardson, D.; Chen, D.; Garrison, C.; Service, D. Potential of colour-infrared digital camera imagery for inventory and mapping of alien plant invasions in South African shrublands. *Int. J. Remote Sens.* **2000**, *21*, 2965–2970. [[CrossRef](#)]

15. Lausch, A.; Heurich, M.; Magdon, P.; Rocchini, D.; Schulz, K.; Bumberger, J.; King, D.J. A Range of Earth Observation Techniques for Assessing Plant Diversity. In *Remote Sensing of Plant Biodiversity*; Springer: Cham, Switzerland, 2020; pp. 309–348. [[CrossRef](#)]
16. Thenkabail, P.S. Characterization of the alternative to slash-and-burn benchmark research area representing the Congolese rainforests of Africa using near-real-time SPOT HRV data. *Int. J. Remote Sens.* **1999**, *20*, 839–877. [[CrossRef](#)]
17. Joshi, C.; De Leeuw, J.; van Andel, J.; Skidmore, A.K.; Lekhak, H.D.; van Duren, I.C.; Norbu, N. Indirect remote sensing of a cryptic forest understorey invasive species. *For. Ecol. Manag.* **2006**, *225*, 245–256. [[CrossRef](#)]
18. Holmes, P.M.; Richardson, D.M.; Esler, K.J.; Witkowski, E.T.; Fourie, S. A decision-making framework for restoring riparian zones degraded by invasive alien plants in South Africa. *South Afr. J. Sci.* **2005**, *101*, 553–564.
19. Rowlinson, L.C.; Summerton, M.; Ahmed, F. Comparison of remote sensing data sources and techniques for identifying and classifying alien invasive vegetation in riparian zones. *Water SA* **1999**, *25*, 497–500.
20. Underwood, E.C.; Ustin, S.L.; Ramirez, C.M. A spatial and spectral image resolution comparison for mapping invasive plants in coastal California. *Environ. Manag.* **2007**, *39*, 63–83. [[CrossRef](#)] [[PubMed](#)]
21. Hamuda, E.; Glavin, M.; Jones, E. A survey of image processing techniques for plant extraction and segmentation in the field. *Comput. Electron. Agric.* **2016**, *125*, 184–199. [[CrossRef](#)]
22. Hunt, E.R.; Hively, W.D.; Mccarty, G.W.; Daughtry, C.S.T.; Forrestal, P.J.; Kratochvil, R.J.; Carr, J.L.; Allen, N.F.; Fox-Rabinovitz, J.R.; Miller, C.D. NIR-Green-Blue High-Resolution Digital Images for Assessment of Winter Cover Crop Biomass. *GIScience Remote Sens.* **2011**, *48*, 86–98. [[CrossRef](#)]
23. Alavipanah, S.; Matinfar, H.; Emam, A.R.; Khodaei, K.; Bagheri, R.H.; Panah, A.Y. Criteria of selecting satellite data for studying land resources. *Desert* **2010**, *15*, 83–102. [[CrossRef](#)]
24. Zurell, D.; Franklin, J.; König, C.; Bouchet, P.J.; Dormann, C.F.; Elith, J.; Fandos, G.; Feng, X.; Guillera-Aroita, G.; Guisan, A.; et al. A standard protocol for reporting species distribution models. *Ecography* **2020**, *43*, 1261–1277. [[CrossRef](#)]
25. Keith, B.D.A. Sampling designs, field techniques and analytical methods for systematic plant population surveys. *Ecol. Manag. Restor.* **2000**, *1*, 125–139. [[CrossRef](#)]
26. Srivastava, V.; Lafond, V.; Griess, V.C. Species distribution models (SDM): Applications, benefits and challenges in invasive species management. *CABI Rev.* **2019**, *14*, 1–13. [[CrossRef](#)]
27. He, K.S.; Bradley, B.A.; Cord, A.F.; Rocchini, D.; Tuanmu, M.-N.; Schmidtlein, S.; Turner, W.; Wegmann, M.; Pettorelli, N. Will remote sensing shape the next generation of species distribution models? *Remote Sens. Ecol. Conserv.* **2015**, *1*, 4–18. [[CrossRef](#)]
28. Rocchini, D.; Andreo, V.; Förster, M.; Garzon-Lopez, C.X.; Gutierrez, A.P.; Gillespie, T.W.; Hauffe, H.C.; He, K.S.; Kleinschmit, B.; Mairota, P.; et al. Potential of remote sensing to predict species invasions: A modelling perspective. *Prog. Phys. Geogr.* **2015**, *39*, 283–309. [[CrossRef](#)]
29. Truong, T.T.A.; Hardy, G.E.S.J.; Andrew, M.E. Contemporary Remotely Sensed Data Products Refine Invasive Plants Risk Mapping in Data Poor Regions. *Front. Plant Sci.* **2017**, *8*, 770. [[CrossRef](#)] [[PubMed](#)]
30. Dormann, C.F.; Schymanski, S.J.; Cabral, J.; Chuine, I.; Graham, C.; Hartig, F.; Kearney, M.; Morin, X.; Römermann, C.; Schröder, B.; et al. Correlation and process in species distribution models: Bridging a dichotomy. *J. Biogeogr.* **2012**, *39*, 2119–2131. [[CrossRef](#)]
31. Kearney, M. Habitat, environment and niche: What are we modelling? *Oikos* **2006**, *115*, 186–191. [[CrossRef](#)]
32. Kumar Rai, P.; Singh, J. Invasive alien plant species: Their impact on environment, ecosystem services and human health. *Ecol. Indic.* **2020**, *111*, 106020. [[CrossRef](#)]
33. Roger, E.; Duursma, D.E.; Downey, P.O.; Gallagher, R.V.; Hughes, L.; Steel, J.; Johnson, S.B.; Leishman, M.R. A tool to assess potential for alien plant establishment and expansion under climate change. *J. Environ. Manag.* **2015**, *159*, 121–127. [[CrossRef](#)]
34. Divišek, J.; Chytrý, M.; Beckage, B.; Gotelli, N.J.; Lososová, Z.; Pyšek, P.; Richardson, D.M.; Molofsky, J. Similarity of introduced plant species to native ones facilitates naturalization, but differences enhance invasion success. *Nat. Commun.* **2018**, *9*, 4631. [[CrossRef](#)]
35. Joshi, C.; De Leeuw, J.; Van Duren, I. Remote sensing and GIS applications for mapping and spatial modeling of invasive species. *ISPRS* **2004**, *35*, B7.
36. Rouget, M.; Richardson, D.M.; Nel, J.L.; Le Maitre, D.C.; Egoh, B.; Mgidi, T. Mapping the potential ranges of major plant invaders in South Africa, Lesotho and Swaziland using climatic suitability. *Divers. Distrib.* **2004**, *10*, 475–484. [[CrossRef](#)]
37. Schnase, J.L.; Carroll, M.L. Automatic variable selection in ecological niche modeling: A case study using Cassin's Sparrow (*Peucaea cassinii*). *PLoS ONE* **2022**, *17*, e0257502. [[CrossRef](#)] [[PubMed](#)]
38. Crowley, M.A.; Cardille, J.A. Remote Sensing's Recent and Future Contributions to Landscape Ecology. *Curr. Landsc. Ecol. Rep.* **2020**, *5*, 45–57. [[CrossRef](#)]
39. Xie, Y.; Sha, Z.; Yu, M. Remote sensing imagery in vegetation mapping: A review. *J. Plant Ecol.* **2008**, *1*, 9–23. [[CrossRef](#)]
40. Wallington, T.J.; Hobbs, R.J.; Moore, S.A. Implications of Current Ecological Thinking for Biodiversity Conservation: A Review of the Salient Issues. *Ecol. Soc.* **2005**, *10*, 15. [[CrossRef](#)]
41. Royle, J.A.; Chandler, R.B.; Yackulic, C.; Nichols, J.D. Likelihood analysis of species occurrence probability from presence-only data for modelling species distributions. *Methods Ecol. Evol.* **2012**, *3*, 545–554. [[CrossRef](#)]
42. Adhikari, U.; Nejadhashemi, A.P.; Woznicki, S.A. Climate change and eastern Africa: A review of impact on major crops. *Food Energy Secur.* **2015**, *4*, 110–132. [[CrossRef](#)]
43. Elith, J.; Phillips, S.J.; Hastie, T.; Dudík, M.; Chee, Y.E.; Yates, C.J. A statistical explanation of MaxEnt for ecologists. *Divers. Distrib.* **2011**, *17*, 43–57. [[CrossRef](#)]

44. Raes, N.; Aguirre-Gutiérrez, J.; Hoorn, C.; Perrigo, A.; Antonelli, A. Modeling framework to estimate and project species distributions space and time. In *Mountains, Climate and Biodiversity*; John Wiley & Sons Ltd.: Hoboken, NJ, USA, 2018; pp. 309–320.
45. Turner, W.; Spector, S.; Gardiner, N.; Fladeland, M.; Sterling, E.; Steininger, M. Remote sensing for biodiversity science and conservation. *Trends Ecol. Evol.* **2003**, *18*, 306–314. [[CrossRef](#)]
46. Xie, Y.; Zhang, A.; Welsh, W. Mapping Wetlands and Phragmites Using Publically Available Remotely Sensed Images. *Photogramm. Eng. Remote Sens.* **2015**, *81*, 69–78. [[CrossRef](#)]
47. Underwood, E.C.; Mulitsch, M.J.; Greenberg, J.; Whiting, M.L.; Ustin, S.; Kefauver, S. Mapping Invasive Aquatic Vegetation in the Sacramento-San Joaquin Delta using Hyperspectral Imagery. *Environ. Monit. Assess.* **2006**, *121*, 47–64. [[CrossRef](#)]
48. Kruger, A.C.; Shongwe, S. Temperature trends in southern Africa: 1960–2003. *Int. J. Climatol. A J. R. Meteorol. Soc.* **2004**, *24*, 1929–1945. [[CrossRef](#)]
49. Mpandeli, S. Managing Climate Risks Using Seasonal Climate Forecast Information in Vhembe District in Limpopo Province, South Africa. *J. Sustain. Dev.* **2014**, *7*, 68. [[CrossRef](#)]
50. Van Wyk, A.E.; Smith, G.F. *Regions of Floristic Endemism in Southern Africa: A Review with Emphasis on Succulents*; Umdaus Press: Hartfield, South Africa, 2001.
51. Holden, P.B.; Rebelo, A.J.; New, M.G. Mapping invasive alien trees in water towers: A combined approach using satellite data fusion, drone technology and expert engagement. *Remote Sens. Appl. Soc. Environ.* **2020**, *21*, 100448. [[CrossRef](#)]
52. Desmet, P.G.; Holness, S.; Skowno, A.; Egan, V.T. Limpopo Conservation Plan v.2: Technical Report. Contract Number EDET/2216/2012. Report for Limpopo Department of Economic Development, Environment & Tourism (LEDET) by ECOSOL GIS. 2013. Available online: https://conservationcorridor.org/cpb/Desmet_et_al_2013.pdf (accessed on 15 March 2023).
53. Kuching, S. The performance of maximum likelihood, spectral angle mapper, neural network and decision tree classifiers in hyperspectral image analysis. *J. Comput. Sci.* **2007**, *3*, 419–423.
54. De Carvalho, O.A.; Meneses, P.R. Spectral correlation mapper (SCM): An improvement on the spectral angle mapper (SAM). In Proceedings of the Summaries of the 9th JPL Airborne Earth Science Workshop, Pasadena, CA, USA, 23–25 February 2000; JPL Publication: Pasadena, CA, USA, 2000; Volume 9, p. 2.
55. Exelis Visual Information Solutions. ENVI Pocket Guide Volume 1, 2 & 3. Boulder, Colorado: Exelis Visual Information Solutions. Pages Used. 2013. Available online: [https://www.scirp.org/\(S\(i43dyn45teexjx455qlt3d2q\)\)/reference/ReferencesPapers.aspx?ReferenceID=1857492](https://www.scirp.org/(S(i43dyn45teexjx455qlt3d2q))/reference/ReferencesPapers.aspx?ReferenceID=1857492) (accessed on 15 March 2023).
56. Sparrow, B.D.; Edwards, W.; Munroe, S.; Wardle, G.M.; Guerin, G.R.; Bastin, J.; Morris, B.; Christensen, R.; Phinn, S.; Lowe, A.J. Effective ecosystem monitoring requires a multi-scaled approach. *Biol. Rev.* **2020**, *95*, 1706–1719. [[CrossRef](#)]

Disclaimer/Publisher’s Note: The statements, opinions and data contained in all publications are solely those of the individual author(s) and contributor(s) and not of MDPI and/or the editor(s). MDPI and/or the editor(s) disclaim responsibility for any injury to people or property resulting from any ideas, methods, instructions or products referred to in the content.